Dynamic contrast-enhanced magnetic resonance imaging of radiation therapy-induced microcirculation changes in rectal cancer

Int. J. Radiation Oncology Biol. Phys., Vol. 63, No. 5, pp. 1309–1315, 2005

0360-3016/05/$–see front matter

ELSEVIER

doi:10.1016/j.ijrobp.2005.04.052

CLINICAL INVESTIGATION **Colorectum**

DYNAMIC CONTRAST-ENHANCED MAGNETIC RESONANCE IMAGING OF RADIATION THERAPY-INDUCED MICROCIRCULATION CHANGES IN RECTAL CANCER

Quido G. de Lussanet, M.D.*† Walter H. Backes, Ph.D.,* Arjan W. Griffioen, Ph.D.,‡§ Anwar R. Padhani, M.B., B.S.,‖ Coen I. Baeten, M.D.,‡§ Angela van Baardwijk, M.D.,§¶ Philippe Lambin, M.D., Ph.D.,§¶ Geerard L. Beets, M.D., Ph.D.,# Jos M. A. van Engelshoven, M.D., Ph.D.,*† and Regina G. H. Beets-Tan, M.D., Ph.D.*‡

Departments of *Radiology, ¶Radiation Therapy, Maastro Clinic, and #Surgical Oncology; †Cardiovascular Research Institute Maastricht (CARIM) and §Research Institute for Growth and Development (GROW), Maastricht University, Maastricht, The Netherlands; ‡Angiogenesis Laboratory, Department of Pathology and Internal Medicine, Maastricht University Hospital, Maastricht, The Netherlands; ‖Paul Strickland Scanner Centre, Mount Vernon Hospital, Northwood, Middlesex, UK

Purpose: Dynamic contrast-enhanced T1-weighted magnetic resonance imaging (DCE-MRI) allows noninvasive evaluation of tumor microvasculature characteristics. This study evaluated radiation therapy related microvascular changes in locally advanced rectal cancer by DCE-MRI and histology.

Methods and Materials: Dynamic contrast-enhanced-MRI was performed in 17 patients with primary rectal cancer. Seven patients underwent 25 fractions of 1.8 Gy radiation therapy (RT) (long RT) before DCE-MRI and 10 did not. Of these 10, 3 patients underwent five fractions of 5 Gy RT (short RT) in the week before surgery. The RT treated and nontreated groups were compared in terms of endothelial transfer coefficient (K^{PS}, measured by DCE-MRI), microvessel density (MVD) (scored by immunoreactivity to CD31 and CD34), and tumor cell and endothelial cell proliferation (scored by immunoreactivity to Ki67).

Results: Tumor K^{PS} was 77% ($p = 0.03$) lower in the RT-treated group. Histogram analyses showed that RT reduced both magnitude and intratumor heterogeneity of K^{PS} ($p = 0.01$). MVD was significantly lower (37%, $p = 0.03$) in tumors treated with long RT than in nonirradiated tumors, but this was not the case with short RT. Endothelial cell proliferation was reduced with short RT (81%, $p = 0.02$) just before surgery, but not with long RT ($p > 0.8$). Tumor cell proliferation was reduced with both long (57%, $p < 0.001$) and short RT (52%, $p = 0.002$).

Conclusion: Dynamic contrast-enhanced-MRI–derived K^{PS} values showed significant radiation therapy related reductions in microvessel blood flow in locally advanced rectal cancer. These findings may be useful in evaluating effects of radiation combination therapies (e.g., chemoradiation or RT combined with antiangiogenesis therapy), to account for effects of RT alone. © 2005 Elsevier Inc.

Rectal cancer, Radiation therapy, Magnetic resonance imaging, Angiogenesis, Tumor perfusion.

INTRODUCTION

Dynamic contrast-enhanced magnetic resonance imaging (DCE-MRI) combined with pharmacokinetic modeling is a promising noninvasive imaging technique for evaluating tumor microvasculature (1, 2). Although conventional MRI allows qualitative tumor characterization (e.g., size and contrast agent uptake) (3–5), combining DCE-MRI with general pharmacokinetic tracer-exchange analysis produces physiologic parameters that allow functional characterization of changes in the tumor microvasculature (e.g., tumor angiogenesis) (6–8).

In rectal cancer patients, DCE-MRI–derived parameters have been shown to change early during the course of radiation therapy (RT) (9) and to be related to the tumor response to chemoradiation combination therapy (10, 11). Few studies have looked at tumor microvascular characteristics after RT alone, and none have good correlation with histology. In animal tumor models, a DCE-MRI–derived parameter for tumor blood flow, the endothelial transfer coefficient (K^{PS}), was shown to be related to immunohistochemical microvessel density scores (MVD) (12, 13) and to be useful for detecting effects of antivascular treatments (14–16). Although RT-related antivascular effects are a

Reprint requests to: Quido G. de Lussanet, M.D., Department of Radiology, Maastricht University Hospital, P.O. Box 5800, 6202AZ Maastricht, The Netherlands. Tel: (+31) 43-387-6910 (-4910); Fax: (+ 31) 43-387-6909; E-mail: qdlu@rdia.azm.nl

Received Feb 9, 2005, and in revised form April 20, 2005. Accepted for publication April 25, 2005.

generally accepted phenomenon (17), the extent to which RT affects the DCE-MRI–derived K^{PS} in locally advanced rectal cancer, for example, is unknown. Because RT is increasingly being administered in combination with chemotherapy or experimental therapies, including antivascular agents (18), and DCE-MRI is becoming an accepted noninvasive surrogate marker for evaluating antivascular effects of these combination therapies, possible RT-related effects on DCE-MRI–derived parameters need to be assessed.

The purpose of this study was to evaluate the effects of neoadjuvant RT in patients with locally advanced rectal cancer by DCE-MRI and to correlate changes in DCE-MRI with immunohistochemical analysis of tumor vascularization and proliferation of tumor cells and endothelial cells.

PATIENTS AND METHODS

Patients and treatment

The ethical review board of our institute approved this study, and all patients gave written informed consent. DCE-MRI was performed in 17 patients (median age, 63 ± 6 years [SD]) with curable primary locally advanced rectal cancer. Twelve patients were male and 5 were female (3 in the long-RT group and 2 in the group without RT). Radiation therapy regimens were allocated by the attending clinicians, who were not involved in the DCE-MRI or histologic data acquisition and analysis. Seven patients underwent a long course of 25 fractions (25 × 1.8 Gy, total 45 Gy) preoperative RT (indicated here as long RT) before DCE-MRI, whereas 10 patients did not. Three of these 10 patients, however, underwent a short course of five fractions (5 × 5 Gy, total 25 Gy) preoperative RT (short RT) in the week before surgery. Because there is a potential difference in effect between short RT and long RT, the 3 patients with short RT were analyzed as a separate group for the histologic analyses after surgery. Obviously, the time between the start of RT and surgery was significantly ($p < 0.001$) longer for long RT (SD, 46 ± 16 days) than for short RT (8 ± 2). The average time between MRI and surgery was not significantly different ($p > 0.4$) between the patients with long RT (SD, 18 ± 13 days), those without RT (25 ± 20), or those with short RT (24 ± 20).

MRI

Dynamic contrast-enhanced magnetic resonance imaging was performed with a conventional clinical MRI scanner at 1.5 Tesla (Intera, Philips, Best, The Netherlands), with a five-element cardiac phased array coil. DCE-MRI included six precontrast T1-weighted measurements (3D fast-field echo, TR 8.0 ms, echo time 3.9 ms, 10 axial slices [slice thickness, 8 mm], field-of-view 290 × 290 mm, matrix 128 × 128) with different flip angles (FAs) (2°, 5°, 10°, 15°, 25°, and 35°) to determine the T1 relaxation time in the blood and tissue before contrast agent arrival, on a pixel-by-pixel basis (19). This was followed by the dynamic contrast-enhanced series using the same sequence but with an FA of 35° only (250 scans of 2.4 s), for a total duration of 10 min. Gadopentetate dimeglumine (Schering AG, Berlin, Germany; 0.15 mmol/kg body weight) was injected intravenously (3 mL/s) and flushed with 15 mL saline (3 mL/s) at the start of the eighth dynamic scan.

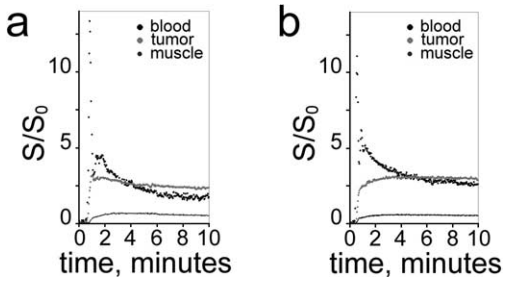

Fig. 1. Representative (i.e., median endothelial transfer coefficient) signal intensity time courses measured with dynamic contrast-enhanced magnetic resonance imaging in a tumor without radiation therapy (RT) (a) show that its increase in signal intensity directly after contrast injection is smaller but similar to the steep signal increase in the blood including the small recirculation peak. Conversely, in a tumor with long RT (b), the signal intensity increase is slower and prolonged, unlike the blood signal, and the decline in tumor signal is substantially slower than in the tumor without RT.

MRI data analysis

Magnetic resonance imaging data were analyzed using a general kinetic two-compartment exchange model as described, for example, by Daldrup *et al.* (6, 13). Briefly, local T1 relaxation rates of the precontrast time-averaged images and contrast-enhanced image signal intensity time courses (Fig. 1) were used to determine the concentrations of contrast medium in the blood plasma (common femoral arteries), tumor, and gluteus maximus muscle. An experienced gastrointestinal radiologist defined the tumor volume region of interest on the T1-weighted images. Application of the general kinetic model (6, 13) yielded the K^{PS}, the reflux rate (k), both expressed as mL/min/100 cm^3 of tissue, and the plasma fraction (f^{PV}) values as mL/100 cm^3 of tissue. Dividing K^{PS} by k yielded the volume fraction of the extravascular extracellular space (EES). Values of K^{PS}, f^{PV}, and EES in individual voxels were collected for tumor histogram analysis (20, 21) and to determine the median tumor values and median tumor/muscle ratios. Intratumor heterogeneity was assessed by the 95th percentile tumor values.

The tumor perfusion index (PI) (mL/min/100 cm^3 of tissue) was also calculated according to the method described by de Vries *et al.* (11). PI is the maximum of the temporal derivative of the temporal changes in T1-relaxation rate divided by the corresponding T1-relaxation rate change early after contrast injection.

Histology and immunohistochemistry

Serial sections (thickness 5 μm) from the most invasive tumor area were used for immunohistochemical stainings to determine MVD, and endothelial cell and tumor cell proliferation was assessed by double staining with a mixture of Ki-67 antibody (rabbit anti-human, Clone SP6, Laboratory Vision, Fremont, CA) and mouse anti-human CD31 (Dako, Glostrup, Denmark) in combination with mouse QBEND-10 anti-CD34 (Monosan, Uden, Netherlands). Ki-67 antibody was detected by biotin-labeled swine anti-rabbit IgG (Dako), incubated with avidine-biotin complex HRP (Dako) and developed with diaminobenzidine (DAB, Sigma). CD31 and CD34 were detected by alkaline phosphatase labeled goat anti-mouse IgG (Dako). The sections were mounted in imsol (Imsol-Mount, Klinipath, Duiven, The Netherlands).

Microvessel density scores (CD31/CD34+ vessels) and endo-

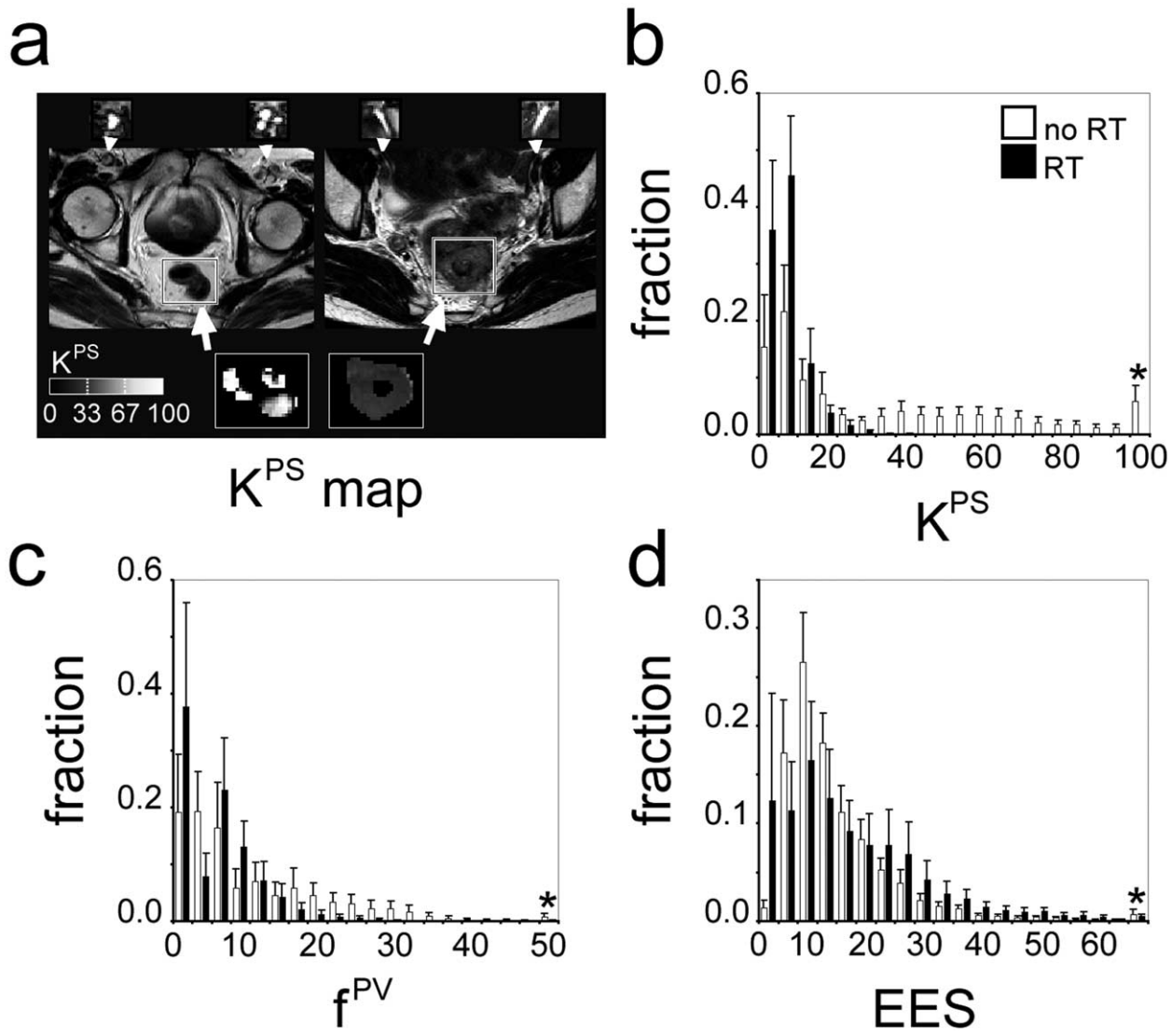

Fig. 2. (a) Axial T2-weighted images were used to locate the tumor. Shown here are tumors with the median endothelial transfer coefficient (K^{PS}) without radiation therapy (RT) (left) and with long RT (right); the top inserts illustrate the signal enhancement in the common femoral arteries directly after contrast injection on the corresponding T1-weighted acquisition; the bottom inserts are the gray scale–coded tumor K^{PS} maps, which illustrate that K^{PS} is lower in magnitude and heterogeneity after long RT. Averaged histogram distribution plots for all tumors show that (b) K^{PS} and (c) plasma fraction (f^{PV}) are lower and less heterogeneous (i.e., smaller intertumor variation) in tumors with long RT (black bars) than in tumors without RT (white bars); whereas (d) extravascular extracellular space (EES) is just slightly increased in tumors with long RT. The error bars (SEM) illustrate the intertumor variation. *Indicates that the highest values (K^{PS} >95.0, EES >63.3, and f^{PV} >47.5) were pooled.

thelial cell proliferation (CD31/CD34 and Ki67+) were determined independently by two observers along a predefined line from the luminal side of the tumor to the deepest invasion, as the total number of vessels divided by the area (number of 0.22 mm^2 optic fields). The endothelial cell proliferation ratio was calculated by dividing the number of proliferating endothelial cells by the MVD. The ratio of the number of Ki67+ tumor cells and the total number of tumor cells in the predefined line was scored as 1 (<25%), 2 (25–75%), or 3 (>75%). The total number of Ki-67+ tumor cells/mm^2 was counted in three predefined Ki-67 hot spots (optic field, 0.22 mm^2).

Statistical methods

Differences in histologic and immunohistochemical scores and median DCE-MRI parameters between the groups with and without RT were compared using the two-sample (two-tailed) Student *t* test. The Pearson correlation coefficient (*r*) was calculated to reveal a possible relationship between tumor PI and K^{PS} values. Statistical significance was inferred at the $p < 0.05$ level.

RESULTS

DCE-MRI findings

All patients underwent DCE-MRI without difficulties in the imaging procedures.

A slower "leakage" of contrast medium into the tumor was found (a difference of 77% [$p = 0.03$]) in patients who had received RT, as assessed by the endothelial transfer coefficient K^{PS} (Fig. 1 and 2a, and Table 1). Histogram

Table 1. DCE-MRI derived parameters

		Tumor values		
		Median	95th percentile	Tumor:muscle ratio
K^{PS}	No RT	28.6 ± 26.8	67.8 ± 55.2	6.5 ± 6.3
	Long RT	6.5 ± 2.4	15.4 ± 4.1	1.5 ± 1.0
f^{PV}	No RT	2.3 ± 2.0	1.8 ± 1.7	—
	Long RT	1.4 ± 1.1	1.2 ± 0.9	—
EES	No RT	0.39 ± 0.15	0.31 ± 0.15	1.3 ± 0.3
	Long RT	0.43 ± 0.11	0.35 ± 0.13	2.1 ± 1.3

Abbreviations: DCE = MRI/dynamic contrast-enhanced; K^{PS} = endothelial transfer coefficient; f^{PV} = plasma fraction; EES = extravascular extracellular space; RT = radiation therapy.

analysis of all tumor pixel K^{PS} values yielded lower ranges of K^{PS} measured in tumors with RT than in tumors without RT (Fig. 2b). These lower ranges of tumor K^{PS} values in tumors with RT were reflected by the lower 95th percentile tumor K^{PS} values ($p = 0.02$), and by the tumor:muscle ratio ($p = 0.03$) (Table 1). In contradistinction, K^{PS} in muscle tissue was slightly higher in tumors with RT than in tumors without RT (NS, $p > 0.3$) (median ± SD, 8.1 ± 8.1 after RT, and 4.6 ± 2.8 without RT).

The significant correlation ($r = 0.74$, $p < 0.001$) that was observed between the tumor K^{PS} and the perfusion index (PI) for all tumors combined reflects the overall similarity between these parameters. Unlike K^{PS}, however, PI did not show significant differences in relation to RT ($p = 0.5$) (median PI ± SD was 34 ± 10 after RT, and 39 ± 21 without RT).

Histogram analysis suggested lower f^{PV} values in tumors with RT than in tumors without RT (Fig. 2c). However, these differences were not significant, either for median tumor f^{PV} values ($p = 0.3$) or for 95th percentile values ($p = 0.3$) (Table 1). Because f^{PV} values were very low (sometimes approaching zero), the tumor:muscle f^{PV} ratio did not result in realistic values and was therefore not calculated.

No significant ($p > 0.4$) changes were observed in tumor EES values. Tumor:muscle ratios were, however, about twice as high (NS, $p > 0.1$) in tumors with RT than in tumors without RT (Table 1, Fig. 2d).

Histologic findings

Tumor cell proliferation was significantly lower ($p = 0.0006$) in the tumors that were treated with long RT than in those not treated with RT; lower tumor cell proliferation was also observed in the three tumors treated with short RT ($p = 0.02$) (Fig. 3a).

The long RT regimen resulted in significantly ($p = 0.03$) lower MVD scores compared with the nonirradiated tumors (Fig. 3b), but the short RT regimen did not. Endothelial cell proliferation ratios were significantly ($p < 0.05$) lower after the short RT regimen, which had been administered during the week before surgery, as compared with nonirradiated tumors, but not after the long RT ($p > 0.8$), which had been administered in the course of several weeks before surgery (Fig. 3c).

DISCUSSION

The results of this study demonstrate significant RT-related microcirculation changes in locally advanced rectal cancer, as assessed by DCE-MRI and histology.

The DCE-MRI derived K^{PS}, measured using a low molecular-weight contrast agent, largely reflects tumor blood flow, as well as the leakiness (i.e., microvessel permeability surface area product) of the tumor microvessels (21, 22). Therefore, K^{PS} was effective in showing effects of long RT that occur approximately 2–4 weeks after the initiation of RT (17).

Radiation Therapy damages all blood vessels, but specific effects depend on vessel size, location, and dose–time–volume factors (17). Although acute effects of RT are marked by increased microvascular permeability, related to endothelial cell damage and local inflammation, longer term effects are marked by decreased permeability, resulting

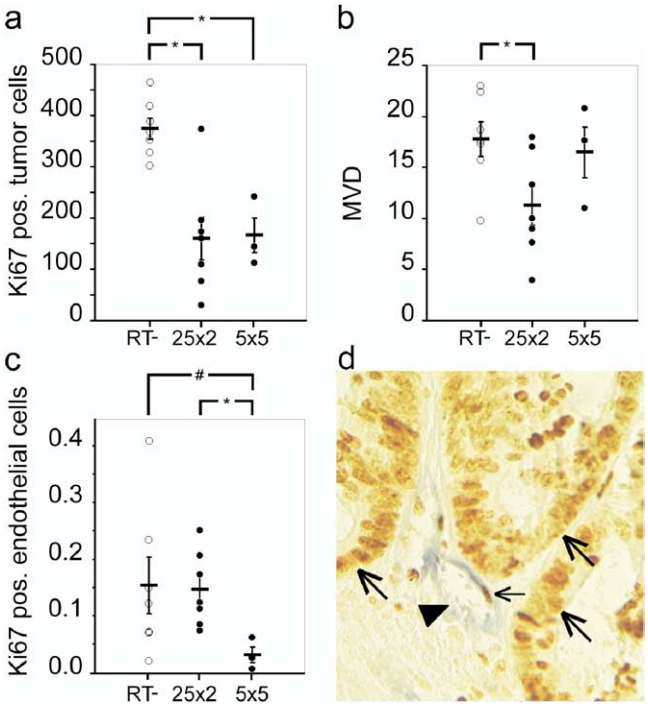

Fig. 3. (a) The average number of Ki-67+ tumor cells was significantly (*) higher in tumors without radiation therapy (RT−) than in tumors irradiated with long RT and short RT; (b) microvessel density (MVD) was significantly (*) lower only after long RT (with respect to RT−); (c) Ki-67 endothelial cell proliferation ratio was lower only after short RT; (d) tumor cell proliferation is marked by the brown, nuclear staining of tumor cells (to Ki67) (large diagonal arrows); the arrowheads depict tumor blood vessels (blue, staining of endothelial cells to CD31 and CD34); note the brown staining of the typical elongated nucleus in an endothelial cell (blue), suggesting angiogenic endothelial cell proliferation in the tumor without RT (small horizontal arrow). Significant differences are indicated by *($p < 0.02$) and #($p < 0.05$). The magnification in (d) is 400×.

from basement membrane thickening and extracapillary fibrosis (17). Additional chronic effects of RT are the inhibition of capillary sprouting and vascular remodeling (23), reduced MVD, endothelial cell destruction, and reduced microvessel functionality as a result of mural thrombi and obliteration of the vessel lumen (17).

K^{PS} is expected to be a more successful marker than other DCE-MRI derived markers, such as PI and area under the signal-intensity-time curve, because K^{PS} represents a single microcirculatory parameter, whereas PI is a perfusion parameter that depends not only on K^{PS}, but is also confounded by (nonsignificant) changes in f^{PV} and EES (22). For example, our study showed a significant (77%) reduction in K^{PS}, whereas PI was reduced by only 15% (which was nonsignificant), despite the strong positive relationship between PI and K^{PS}. De Vries *et al.* (9) reported increases in PI during the first weeks of RT in rectal cancer, which corresponds very well with reported acute effects of RT (17). The reported increases in PI were 25% at most, and the observed possible decline in PI after the final (fourth) week of RT was not significant (9).

Presenting the true tumor K^{PS} may be preferable over the tumor:muscle K^{PS} ratio, because effects of RT in muscle are uncertain. The gluteus maximus muscle, for example, is several centimeters posterior to the rectal tumor, but is still at least partially within anteroposterior field of radiation. Although muscle is generally assumed to produce minimal response to clinical irradiation, transient alterations and varying degrees of atrophy and necrosis have been reported for skeletal muscle after single doses of RT (24). High-dose radical RT can cause persistent muscle edema, often visible on MRI, probably reflecting long-term damage to muscle microcirculation. The increase in muscle K^{PS} observed in the current study did not affect the observed statistical differences in tumor K^{PS} in relation to therapy when expressed as a tumor:muscle ratio.

The DCE-MRI derived volume fraction of the EES showed some increased intratumor variation after RT. Cell destruction caused by radiation may have increased the relative extracellular volume to which the contrast agent can leak, hence increasing EES. In other parts of the tumor, infiltration of inflammatory cells and tissue fibrosis (25) may have decreased EES.

Immunohistochemistry results reflected the antitumor and antiangiogenesis effects of RT. Direct measures of antiangiogenesis effects are reduced MVD and reduced Ki67 immunoreactivity of endothelial cells. Our data show incongruous effects between long and short RT, although it should be noted that the number of patients who underwent short RT was limited. Explanations why short RT yielded low endothelial cell proliferation without differences in MVD, whereas long RT yielded low MVD without differences in endothelial cell proliferation, as compared with nonirradiated tumors, might be related to the higher fraction dosage with short RT or the shorter time interval between RT and surgery with short RT, compared with long RT. Despite lower fraction dosages, long RT may have had short-term effects on endothelial cell proliferation, but endothelial cell proliferation may have recovered during the time interval between RT and surgery, especially because the fraction dosages were lower (26). Because the time between the completion of RT and surgery was less than a week for short RT and several weeks for long RT, it is also possible that in the short RT patients, we were observing the acute effects, such as endothelial cell damage with reduced proliferation, whereas in the long RT patients, we were observing the long-term effects, including endothelial cell destruction and MVD reduction (17).

A larger number of patients would have allowed an evaluation of possible relationships between, for example, K^{PS} and MVD, as demonstrated in animal studies (12, 13). Patient inclusion was stopped because of changes in treatment protocols at our hospital (27, 28). The large intertumor and intratumor variability of K^{PS} values, particularly in the nonirradiated patient group, in combination with the limited number of included patients, hampered strong statistical significance. Future studies should therefore use larger sample sizes to compare patient groups with different treatment regimes (e.g., short RT vs. long RT).

Similarly, colocalizing MRI and histologic parameters might be considered more desirable than our use of one "representative" (e.g., median) value for each parameter. For example, colocalization between K^{PS} and MVD has been demonstrated in animal tumor models, in which the in-plane resolution of MRI (0.5×0.5 mm) matched the optic field of view of the histologic sections; therefore, histologic sections could be closely matched with the MRI sections, and maximum tumor diameters were typically less than 1 cm (14). However, one can imagine the sampling errors that may occur when attempting to colocalize MRI and histology in these large rectal tumors in patients, and the spatial resolution on MRI was substantially lower than that obtained in mice.

Microvessel density is commonly used as a surrogate marker for the tumor microvasculature to validate DCE-MRI derived parameters. However, one important aspect to note is that MVD may not fully equate to the DCE-MRI parameters, because MVD depends on the staining of endothelial cells in blood vessels and is thus a morphologic marker, whereas DCE-MRI derived parameters depend on microcirculatory perfusion and are therefore functional markers.

The antitumor effect of RT was most evident in the reduction of proliferating tumor cells as detected by Ki67 immunoreactivity in tumor cells. This was observed after both long and short RT regimens, and is consistent with earlier reports (29). Although tumor cell immunoreactivity for Ki67 is not a direct measure of angiogenesis in rectal cancer, it might be postulated that RT-related reductions in tumor cell proliferation reduce the production of proangiogenic factors, and thus lead to an angiostatic state.

Clinical implications

Although conventional gadolinium-enhanced MR sequences have limited additional value for morphologic diagnostic assessment of rectal cancer (5), new gadolinium-enhanced MR protocols, such as DCE-MRI, will complement conventional imaging of tissue morphology by noninvasive evaluation of (tumor) tissue physiology. DCE-MRI was used here to show that radiation therapy alone significantly inhibits angiogenesis in rectal cancer. Developments in antiangiogenesis therapy are improving the prospects for anticancer treatment (30, 31), including disseminated colorectal disease (32, 33), when combined with neoadjuvant radiation therapy (18, 34) or chemotherapy (35, 36). The current study provides a reference for future evaluations of additive effects of antiangiogenesis treatments that are supplemented to neoadjuvant radiation therapy in rectal cancer.

REFERENCES

1. McDonald DM, Choyke PL. Imaging of angiogenesis: From microscope to clinic. *Nat Med* 2003;9:713–725.
2. Leach MO, Brindle KM, Evelhoch JL, *et al.* Assessment of antiangiogenic and antivascular therapeutics using MRI: Recommendations for appropriate methodology for clinical trials. *Br J Radiol* 2003;76:S87–S91.
3. Beets-Tan RG, Beets GL, Vliegen RF, *et al.* Accuracy of magnetic resonance imaging in prediction of tumour-free resection margin in rectal cancer surgery. *Lancet* 2001;357:497–504.
4. Beets-Tan RG, Beets GL. Rectal cancer: Review with emphasis on MR imaging. *Radiology* 2004;232:335–346.
5. Vliegen RF, Beets GL, von Meyenfeldt MF, *et al.* Rectal cancer: MR imaging in local staging—Is gadolinium-based contrast material helpful? *Radiology* 2005;234:179–188.
6. Daldrup HE, Shames DM, Husseini W, *et al.* Quantification of the extraction fraction for gadopentetate across breast cancer capillaries. *Magn Reson Med* 1998;40:537–543.
7. Padhani AR. Functional MRI for anticancer therapy assessment. *Eur J Cancer* 2002;38:2116–127.
8. Knopp MV, Von Tengg-Kobligk H, Choyke PL. Functional magnetic resonance imaging in oncology for diagnosis and therapy monitoring. *Mol Cancer Ther* 2003;2:419–426.
9. de Vries A, Griebel J, Kremser C, *et al.* Monitoring of tumor microcirculation during fractionated radiation therapy in patients with rectal carcinoma: Preliminary results and implications for therapy. *Radiology* 2000;217:385–391.
10. George ML, Dzik-Jurasz AS, Padhani AR, *et al.* Non-invasive methods of assessing angiogenesis and their value in predicting response to treatment in colorectal cancer. *Br J Surg* 2001;88:1628–1636.
11. Devries AF, Griebel J, Kremser C, *et al.* Tumor microcirculation evaluated by dynamic magnetic resonance imaging predicts therapy outcome for primary rectal carcinoma. *Cancer Res* 2001;61:2513–2516.
12. van Dijke CF, Brasch RC, Roberts TP, *et al.* Mammary carcinoma model: Correlation of macromolecular contrast-enhanced MR imaging characterizations of tumor microvasculature and histologic capillary density. *Radiology* 1996;198:813–818.
13. de Lussanet QG, Backes WH, Griffioen AW, *et al.* Gadopentetate dimeglumine versus ultrasmall superparamagnetic iron oxide for dynamic contrast-enhanced MR imaging of tumor angiogenesis in human colon carcinoma in mice. *Radiology* 2003;229:429–438.
14. de Lussanet QG, Beets-Tan RG, Backes WH, *et al.* Dynamic contrast-enhanced magnetic resonance imaging at 1.5 Tesla with gadopentetate dimeglumine to assess the angiostatic effects of anginex in mice. *Eur J Cancer* 2004;40:1262–1268.
15. Bhujwalla ZM, Artemov D, Natarajan K, *et al.* Reduction of vascular and permeable regions in solid tumors detected by macromolecular contrast magnetic resonance imaging after treatment with antiangiogenic agent TNP-470. *Clin Cancer Res* 2003;9:355–362.
16. Evelhoch JL, LoRusso PM, He Z, *et al.* Magnetic resonance imaging measurements of the response of murine and human tumors to the vascular-targeting agent ZD6126. *Clin Cancer Res* 2004;10:3650–3657.
17. Byhardt RW, Moss WT. The heart and blood vessels. In: Cox JD, ed. Moss' radiation oncology. 7th ed. St. Louis: Mosby, 1994. p. 311–319.
18. Wachsberger P, Burd R, Dicker AP. Tumor response to ionizing radiation combined with antiangiogenesis or vascular targeting agents: Exploring mechanisms of interaction. *Clin Cancer Res* 2003;9:1957–1971.
19. Haacke M, Brown RW, Thompson MR, Venkatesan R. T1 estimation from SSI measurements at multiple flip angles. In: Venkatesan R, ed. Magnetic resonance imaging: Physical principles and sequence design. New York: John Wiley & Sons, Inc., 1999. p. 654–661.
20. Hayes C, Padhani AR, Leach MO. Assessing changes in tumour vascular function using dynamic contrast-enhanced magnetic resonance imaging. *NMR Biomed* 2002;15:154–163.
21. de Lussanet QG, Langereis S, Beets-Tan RG, *et al.* Relationship between dynamic contrast-enhanced MR imaging kinetic parameters and molecular weight of dendritic contrast agents in tumor angiogenesis in mice. *Radiology* 2005;235:65–72.
22. Tofts PS, Brix G, Buckley DL, *et al.* Estimating kinetic parameters from dynamic contrast-enhanced T(1)-weighted MRI of a diffusable tracer: Standardized quantities and symbols. *J Magn Reson Imaging* 1999;10:223–232.
23. Van Den Brenk HA. The effect of ionizing radiations on capillary sprouting and vascular remodelling in the regenerating repair blastema observed in the rabbit ear chamber. *Am J Roentgenol Radium Ther Nucl Med* 1959;81:859–884.
24. Lewis RB. Changes in striated muscle following single intense doses of x-rays. *Lab Invest* 1954;3:48–55.
25. Dworak O, Keilholz L, Hoffmann A. Pathological features of rectal cancer after preoperative radiochemotherapy. *Int J Colorectal Dis* 1997;12:19–23.
26. Koukourakis MI, Giatromanolaki A, Sivridis E, *et al.* Squamous cell head and neck cancer: Evidence of angiogenic regeneration during radiotherapy. *Anticancer Res* 2001;21:4301–4309.
27. Colorectal Cancer Collaborative Group. Adjuvant radiotherapy for rectal cancer: A systematic overview of 8,507 patients from 22 randomised trials. Lancet 2001;358:1291–1304.
28. Kapiteijn E, Marijnen CA, Nagtegaal ID, *et al.* Preoperative radiotherapy combined with total mesorectal excision for resectable rectal cancer. *N Engl J Med* 2001;345:638–646.
29. Adell G, Zhang H, Jansson A, *et al.* Decreased tumor cell proliferation as an indicator of the effect of preoperative radiotherapy of rectal cancer. *Int J Radiat Oncol Biol Phys* 2001;50:659–663.
30. Carmeliet P, Jain RK. Angiogenesis in cancer and other diseases. *Nature* 2000;407:249–257.
31. Griffioen AW, Molema G. Angiogenesis: Potentials for pharmacologic intervention in the treatment of cancer, cardiovascular diseases, and chronic inflammation. *Pharmacol Rev* 2000;52:237–268.

32. Willett CG, Boucher Y, di Tomaso E, *et al.* Direct evidence that the VEGF-specific antibody bevacizumab has antivascular effects in human rectal cancer. *Nat Med* 2004;10:145–147.
33. Morgan B, Thomas AL, Drevs J, *et al.* Dynamic contrast-enhanced magnetic resonance imaging as a biomarker for the pharmacological response of PTK787/ZK 222584, an inhibitor of the vascular endothelial growth factor receptor tyrosine kinases, in patients with advanced colorectal cancer and liver metastases: Results from two phase I studies. *J Clin Oncol* 2003;21:3955–3964.
34. Dings RP, Williams BW, Song CW, *et al.* Anginex synergizes with radiation therapy to inhibit tumor growth by radiosensitizing endothelial cells. *Cancer Res.* In press.
35. Teicher BA, Sotomayor EA, Huang ZD. Antiangiogenic agents potentiate cytotoxic cancer therapies against primary and metastatic disease. *Cancer Res* 1992;52:6702–6704.
36. Jain RK. Normalizing tumor vasculature with anti-angiogenic therapy: A new paradigm for combination therapy. *Nat Med* 2001;7:987–989.